DOI: 10.13009/EUCASS2017-489

7TH EUROPEAN CONFERENCE FOR AERONAUTICS AND AEROSPACE SCIENCES (EUCASS)

DOI: 489

FEES: a 1/3U Cubesat Mission for In-Orbit Technology Validation

Andrea Colagrossi[⋆†], *Paolo Lunghi*[⋆], *Luca Pompa*[⋆], *Andrea Semprebon*[⋆⋆], *Guido Parissenti*[⋆⋆⋆†] *and Michèle Lavagna*[⋆]

[⋆]*Aerospace Science and Technology Department (DAER), Politecnico di Milano, Milan, Italy*
[⋆⋆]*Electronics, Informatics and Bioengineering Department (DEIB), Politecnico di Milano, Milan, Italy*
[⋆⋆⋆]*GP Advanced Projects Srls, Brescia, Italy*

andrea.colagrossi@polimi.it · guido.parissenti@gpadvancedprojects.com
[†]Corresponding authors

Abstract

The paper presents the development of FEES (Flexible Experimental Embedded Satellite) a pico-platform for in-orbit technology demonstration and validation. The satellite is in the class of the *picosatellites*, with 1/3U dimensions and a mass of 300g. FEES is going to be launched in Mid 2018 with a Falcon 9 launcher. Focus is on critical on-board subsystems, crucial to step over with picosats performances: attitude determination and control, on-board data handling, telecommunication components, among the others, specifically miniaturized for such reduced platforms. In fact, payload and subsystems are packed in a 10x10x3 cm structure which has been designed and produced accordingly.

1. Introduction

Small spacecraft missions are of increasing interest in contemporary space market. In fact, their capabilities to reduce the cost of space access while performing operations, only possible in the past with larger and heavier satellites, are an outstanding achievement of present space technology sector. In the last years, the rising miniaturization of electronic components allowed to integrate fully operational spacecrafts weighing less than a kilogram, which are usually referred to as *picosatellites* or *picosats*.

This paper is intended to present the development of FEES (Flexible Experimental Embedded Satellite), a 1/3U picosat platform to be launched in-orbit in Mid 2018 as piggy back of UNISAT-7 satellite, property of G.A.U.S.S. Srl,[3] with a Falcon 9 launcher. The primary mission objectives of FEES are: in-orbit qualification of an attitude determination and control subsystem (ADCS), together with the relative GNC architecture; in-orbit qualification of commercial GPS receivers; exploitation of IRIDIUM signal to receive data and support on-board traditional radio transmissions architectures. Moreover, FEES aims to test transmission protocols by using Software Defined Radio (SDR) digital technology and perform Earth imaging with a multispectral camera.

The complete set of mission goal of FEES are:

- In-orbit qualification of an ADCS system
- In-orbit qualification of commercial GPS receivers
- Usage of the IRIDIUM global satellite network to receive data, supporting traditional radio transmissions
- In-orbit testing and qualification of a new generation of solar cells
- Measurement of total radiation dose in order to correlate possible electronic and system failures to environmental phenomena
- Testing of various transmission protocols by using Software Defined Radio (SDR) digital technology
- Take pictures of Earth by using a multispectral camera

DOI: 10.13009/EUCASS2017-489

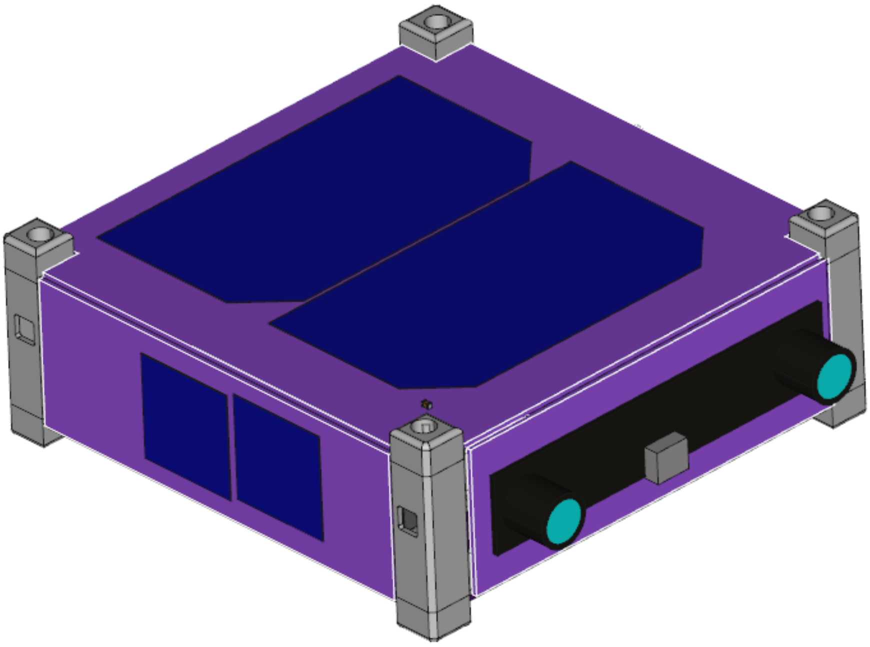

Figure 1: FEES platfom.

The satellite is designed to have all the components on one single inner electronics board, while the externals faces, also made of Printed Circuit Boards (PCB), mounting sensors, actuators and PCB-antennas. The satellite does not have deployable parts or mechanism and its envelope is 300 g, margined, into a $10 \times 10 \times 3$ cm^3 volume.

FEES is going to be injected in a LTDN 10:30 a.m. circular Sun-Synchronous Orbit (SSO) with altitude equal to 575 km. The resulting orbital period is $T = 1.6$ h.

The GNC design aims for a Nadir pointing attitude, while maintaining a suitable Solar Aspect Angle on the body mounted solar cells. The attitude control authority is actuated by 3 PCB-embedded magnetorquers, able to produce, in average between poles and equator, 1×10^{-3} mNm with a power consumption of 0.15 W each. They are 10×10cm^2 coils, composed by 6 layers of 25 turns each and commanded by a PWM voltage regulator. Their performances are completely sufficient for the considered mission, since the expected perturbing torques along the operational orbit are in the order of 5×10^{-5} mNm. The high inclination of the operational sun-synchronous orbit is beneficially exploited to keep control torques available in any direction along the whole orbital period, and the system is not under-actuated, in average, even with magnetic actuators.[13] The attitude determination sensors architecture is composed by gyroscopes, magnetometers, earth sensors, coarse and fine sun sensors and a GPS receiver.

The GNC, realized and tested in Simulink, has to be translated and implemented in C++. The on-board embedded system is an ARM©32-bit Cortex©-M4 microcontroller: due to power and heating constraints its clock has to be reduced, leading to a redesign of the algorithms to better exploit the microcontroller functionalities.
The on-board data handling (OBDH) subsystem functions include the collection and monitoring of on-board sensors data (to be transmitted to ground), the decoding and execution of telecommands received from ground and the execution of ADCS algorithms.
It is also equipped with additional flash memory to host data history: a custom filesystem assures redundancy and robustness to data corruption.

The main electronics components are placed on a mainboard inside the satellite body. Such mainboard, developed by Laser Navigation srl,[5] contains the microcontroller, the power system, the telecommunication systems and the scientific experiments. Sensors and actuators are placed on the satellite external faces.

Telecommunication subsystem is based on different antenna typologies, in order to test and space qualify four different technologies and strategies: traditional 435MHz data link, experimental 1200MHz data link, experimental 435MHz data link with an SDR radio to test multiple transmission concepts, IRIDIUM modem, allowing bidirectional transmission of short amount of data in every part of the world, even though not in view of any ground station. Linkit[6] manages the TT&C development.

Power subsystem will be based on innovative thin solar cells developed and provided by CESI[2] , European leader in manufacturing of solar cells for space application. Moreover, the cubesat will be equipped with experimental high

DOI: 10.13009/EUCASS2017-489

efficiency InGaAs solar cells to be tested and space qualified.

FEES structure consists of a three pieces design aimed to contain the weight, ease the assembly and testing procedure while still ensuring reliability.

FEES represents the joint effort of a number of SMEs and institutions to validate components and concepts to enable a new low cost picosat platform concept. In this endeavour, GP Advanced Projects oversees project management and system engineering activities, other than being the main investor. Politecnico di Milano supports the project with mission analysis, flight dynamics, GNC algorithm design, software on hardware implementation, FDIR definition and provides facilities for environmental tests.

The focus of the paper is on critical on-board subsystems, crucial to step over with picosats performances: attitude determination and control, on-board data handling, telecommunication components, structural elements, among the others, specifically miniaturized for such reduced platforms. Furthermore, the paper describes the smart design adopted to cope with challenges risen in preserving good performance with such reduced size, still ensuring robustness and redundancy. The operations strategies is also discussed, the design of which played a relevant role in sizing the on-board resource request profile. The potential of such a mission, related with the on-board technology TRL increase because of in-orbit testing, is also highlighted.

2. Electronics and Mainboard

The satellite is managed by a STM32L4 microcontroller, with low power mode capabilities. The microcontroller is in charge of managing all the satellite systems. Its main task is to manage the satellite operative modes, which are directly referred to the power systems. The latter is comprised by battery, solar cells and power distribution components. The microcontroller is also in charge of running the GNC/ADCS algorithm, of receiving inputs from the sensors and of commanding the actuators. Another task is to manage the whole TT&C subsystem, comprised of the main TT&C module, its connection with the SDR generating hardware and the IRIDIUM module. Finally, it manages the on-board scientific experiments, meaning the innovative solar cells and a radiation experiment. The microcontroller and the main subsystems components are placed inside the satellite body, on a dedicated motherboard which can represents the heart of a family of spacecraft with the same electronics but different sizes.

3. Attitude Determination and Control Subsystem

The necessity to control and stabilize the attitude dynamics of FEES is fundamental in order to achieve basic mission goals. The low inertia of the spacecraft compared to the high electronics density makes the system totally unstable, because of the strong and time varying interaction with the Earth's magnetic field. Moreover, inertia stabilization techniques are not effective in this case and, thus, an active control system is needed. In particular, FEES has a three-axes and fully magnetic ADCS, especially developed for picosat missions similar to the one presented in this paper.

The primary attitude control requirement is a coarse nadir pointing ($\sim 10°$), needed for the proper operations of the TT&C subsystem and to correctly employ the on-board camera. The power subsystem and the required incoming solar power, have been used to define the secondary pointing requirement, where the solar panels have to be oriented in the direction of the orbital velocity. Furthermore, the spacecraft shall be able to de-tumble soon after the release from the launcher, and shall reach the stabilized nominal condition within few orbits (i.e. $\sim 7-8$ orbits, equivalent to $\sim 12\,\mathrm{h}$ for the considered operational orbit).

3.1 Attitude Control

FEES is equipped with 3 magnetorquers, embedded into the main PCB. No reaction wheel could be placed inside the satellite, due to volume and mass constraints. Thus, a fully magnetic control had to be designed, exploiting the natural geomagnetic field and facing under-actuation in some phases. In fact, the main issue faced with magnetic-only control is the impossibility to actuate a rotation about a direction which is parallel to the local geomagnetic field.[19] The control torque generated by a the magnetorquers is

$$\mathbf{T}_c = -\mathbf{B}_b \times \mathbf{d}_c, \tag{1}$$

where $\mathbf{B}_b$ is the local geomagnetic field, in body frame, and $\mathbf{d}_c$ is the induced magnetic dipole for control purposes. Thus, it is impossible to obtain $\mathbf{T}_c$ parallel to $\mathbf{B}_b$ through a cross product. Although locally under-controllable, the overall attitude dynamics can be controlled along an orbit, since the local geomagnetic field changes direction due to the high inclination. This feature is exploited in tuning the control gains in order to find a control action that guarantees a global controllability, at the cost of local uncontrollability time frames, as described in the following.

DOI: 10.13009/EUCASS2017-489

The control system logic is based on a Proportional-Derivative (PD) action. Two angles are defined for the algorithm:

- The nadir error angle α_n, i.e. the angle between the nadir direction and the vector normal to the nadir pointing surface; when $\alpha_n = 0$, the nadir face correctly point towards the Earth.
- The velocity error angle α_v, i.e. the angle between the velocity direction and the vector normal to the prograde face.

For each of the two error angles one can find the rotation direction; thus, the combination of direction and rotation angle can be transformed into rotation matrices $[A]_n$ and $[A]_v$, respectively. These matrices will be employed to define the guidance of the system.

The proportional action of the controller applies a torque proportional to the error angles, in a direction such that those angles are reduced (ideally, nullified). A different weight is set between nadir and velocity errors, since the former is more important for mission requirements. Let us consider the two error rotation matrices, $[A]_n$ and $[A]_v$; in general, if the angles are small, a rotation matrix may be linearised into

$$[A] = \begin{bmatrix} 1 & e_z & -e_y \\ -e_z & 1 & e_x \\ e_y & -e_x & 1 \end{bmatrix} \tag{2}$$

Thus, the two error rotation matrices provide two sets of small error angles

$$\mathbf{e}_n = [e_{xn}, e_{yn}, e_{zn}]^T \qquad \mathbf{e}_v = [e_{xv}, e_{yv}, e_{zv}]^T \tag{3}$$

related to nadir and velocity direction, respectively. The proportional control torque is then described as follows

$$\mathbf{T}_{c,p} = [K]_n \mathbf{e}_n + [K]_v \mathbf{e}_v \tag{4}$$

where $[K]_n$ and $[K]_v$ are diagonal matrices, that contain the controller gains for each error angle vector element. This allows to set different gains for the different components, enhancing the performance of the controller in respect to the overall behaviour.

The derivative action minimizes the difference between the body angular velocity, and the reference orbital angular velocity $\dot{\boldsymbol{\theta}}$, formalised as follows;

$$\mathbf{T}_{c,d} = K_\omega [\beta](\boldsymbol{\omega} - \dot{\boldsymbol{\theta}}) \tag{5}$$

where $[\beta]$ is a correction coefficient, to avoid singularities in the control logic if a torque parallel to $\mathbf{B}$ is requested. Note that the derivative control gain is a scalar, acting on all three axes, since no beneficial effect was obtained by setting different coefficients on the three angular velocities. Nonetheless, this kind of derivative action was found to be more efficient, since

- In de-tumbling mode, the high angular velocities produce a strong control action, which slows the rotation of the satellite and brings its attitude towards the nominal condition;
- In nominal operation mode, the small deviations in angular velocity may be assumed to coincide with the rates of the small angles, with a first order approximation.

The correction matrix $[\beta]$ is computed as

$$[\beta] = [I] - \frac{\mathbf{B}_b \cdot \mathbf{B}_b^T}{||\mathbf{B}||^2} \tag{6}$$

so that the requested torque has no components along $\mathbf{B}_b$, nullified by $[\beta]$. This strategy is particularly useful in de-tumbling mode, when the magnetic field varies rapidly, and singularities in the algorithm (i.e. requests for a torque impossible to actuate locally) may lead to global instabilities.[10] This simple implementation allows also for a lighter control logic, in terms of software implementation, both on-board and for simulation, at the reasonable price of a slower, non-optimal, although efficient, de-tumbling control.[9]

The main challenge faced during the design of the GNC subsystem was the tuning of the *PD* gains, because of the locally under-actuated system. For this reason, the tuning of the controller gains was not performed with standard techniques, but a long-term horizon controllability was sought, in an integral sense. A merit function $f_m(\mathbf{K})$, where the vector $\mathbf{K}$ contains the 3+3 *P* gains and the *D* gain, was defined as the integral of the error over a number of orbits N

$$f_m(\mathbf{K}) = \int_0^{NT} (\alpha_n + \alpha_v)\, dt, \tag{7}$$

DOI: 10.13009/EUCASS2017-489

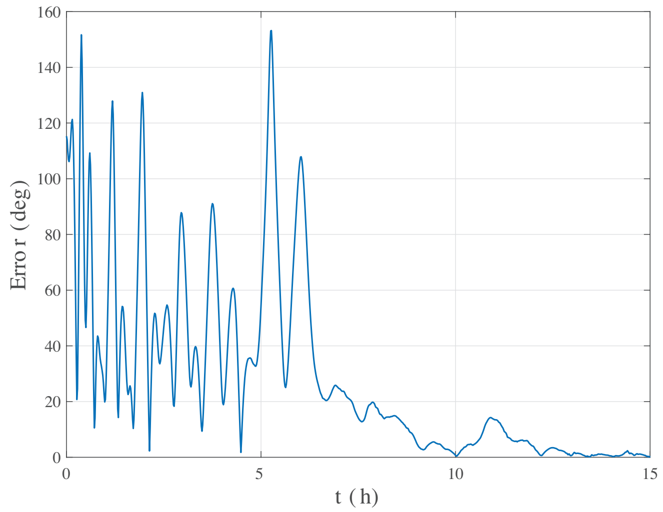

Figure 2: Nominal attitude acquisition.

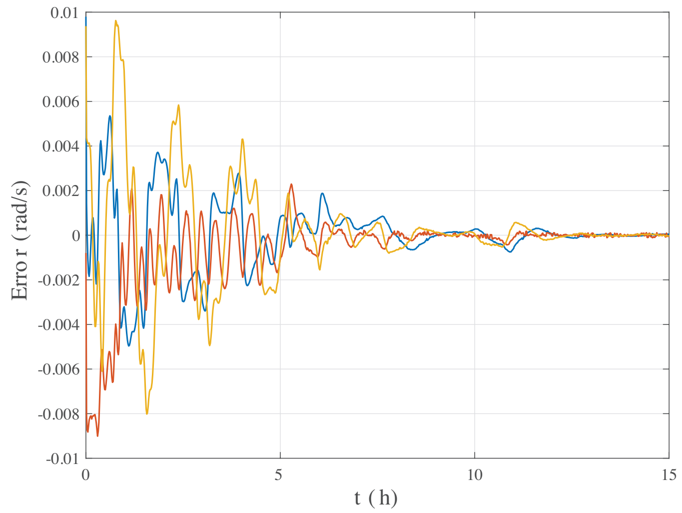

Figure 3: De-tumbling phase: error with respect to the nominal angular velocity.

where T is the orbital period. The choice of the controller gains is thus formulated as a minimization problem, looking for a set $\mathbf{K}$ that minimizes the integral error. Due to the peculiarity of the problem, where the merit function is highly non-linear, the optimization was performed using an heuristic method, namely, a genetic evolutionary algorithm.

The results of the optimization manifest a peculiar behaviour, which is deduced to be a consequence of the magnetic-only control system: after periods of good controllability, the nominal attitude is lost. The unstable system is characterized by a Bode's sensitivity integral that is constant and positive: the reduction in disturbance sensitivity at desired frequency leads to worse performances at higher frequencies. Thus, the closed-loop system interaction with the Earth's magnetic field is affected by the higher order harmonics of the geomagnetic field and the system behaviour is necessarily unstable at some points. Moreover, it has to be remembered that the unstable system is controlled in average along one orbit by a locally under-actuated control system, which in some cases may be not sufficient to maintain the system within the nominal state. However, when accuracy is lost, the spin of the satellite makes stronger the de-tumbling action, which is able to bring it back to nominal operating attitude.

Figure 2 illustrates the nominal attitude acquisition from a random initial condition. In particular, the initial Nadir error angle is $\sim 120°$ and the satellite is tumbling. The ACS is able to de-tumble the spacecraft in ~ 5 orbital periods and correctly align the Nadir face with an error angle in the order of $10°$. These performance are compatible with the requirements for the ADCS described before.

DOI: 10.13009/EUCASS2017-489

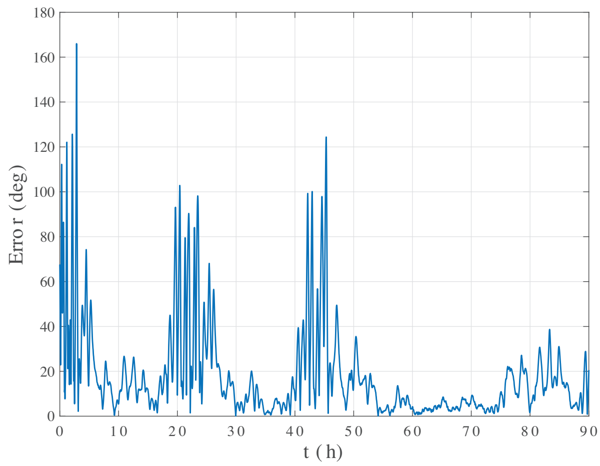

Figure 4: Long-term nadir pointing error.

In fig. 3, the error velocity with respect to the nominal reference condition is represented during a typical detumbling phase. Indeed, also in this case the spacecraft acquires nominal state in less than 5 orbital periods. Then, the ACS is able to maintain the desired state; the only exception is related with the loss of pointing periods.

These loss of pointing periods, when the spacecraft is not correctly oriented, are shown in fig. 4. The picture reports just a sample result, portraying the nadir pointing error over roughly 60 orbits. The periods of control loss are evident, as well as the capability to recover from high errors and acquire nominal pointing accuracy. This pattern in the behaviour is repeated during the nominal lifetime of the satellite. However, the time in which the spacecraft is correctly controlled are sufficient to satisfy the imposed mission requirements.

3.2 Attitude Determination

The attitude determination subsystem is based on a simple and effective architecture, which exploits different sensors that are used together and processed to obtain the orientation of the spacecraft with an accuracy sufficient to satisfy the imposed requirements.

The spacecraft is able to detect the position of the Sun with two different types sensors: photodiodes employed as coarse Sun sensors (with the back-up guaranteed thanks to the presence of the solar panels), CMOS technology and a micrometric hole in the PCB used as fine Sun sensor. The former are installed on each face of FEES, while the latter are only present on the two large faces. The Earth's direction is obtained with two thermopiles mounted on the large face of the spacecraft, acting as two redundant Earth horizon sensors. In addition, the ADS makes also use of a magnetometer that measures the Earth's magnetic field with an accuracy of 200 nT. An inertial measurement unit (IMU) is also available on the spacecraft and the set of sensors is completed with a GPS receiver.

The proposed determination logic is robust enough and it is particularly efficient, with the purpose to be implemented on-board within memory and processor constraints. Indeed, according to system specification, the computing loads for the on-board computer are targeted to be extremely limited, since the available resources are in the class of those typical for a picosatellite (e.g. < 10 DMIPS).

The ADS algorithm starts with the post processing phase of each sensor, determining the desired measured vector in body reference and the quality of the sensor's signal, by associating an index to each measure. Then, all the valid signals are processed by a static attitude determination logic. In this phase a statistical algorithm solves the Wahba's problem.[21] Each sensor is weighted in this step according to the validity index of its measure. The outcome of the statistical attitude determination is combined with the data coming from the IMU and processed with a complementary filter.[20] This filter is very effective and computationally efficient, especially when compared to a classic Kalman filter. The estimation of the spacecraft's orientation is available, in terms of quaternions, $\mathbf{q}$, and of the angular velocity, $\boldsymbol{\omega}$. These estimates are directly sent to the output of the ADS, if all the sensors are properly working with high validity indices. On the contrary, when enough information from the sensors are not available, a propagator is initialized from the last valid attitude state and the dynamics is propagated with the unbiased output of the IMU. In this last case, the output of the ADS is the propagated attitude.

The performances of the designed ADS are satisfactory, in particular with reference to the imposed requirements. The whole determination logic is efficient and can be easily managed by the on-board computer. Many simulations have

DOI: 10.13009/EUCASS2017-489

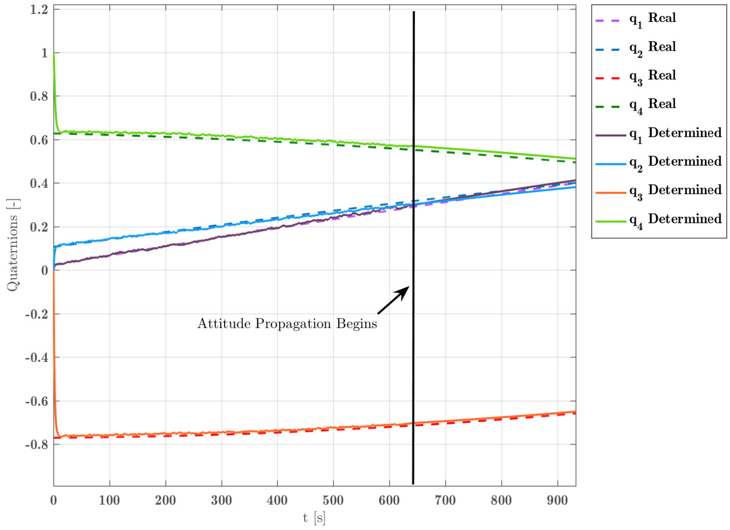

Figure 5: Attitude determination performances, starting from unknown attitude state in terms of quaternions $\mathbf{q}$. (All sensors are operational before the point highlighted by the vertical black line. Then the attitude is propagated because the spacecraft enters in eclipse).

been run, testing and validating the algorithm with the simulated model. Figures 5 and 6 report the performances of the attitude determination logic in the operational orbit, obtained for an example simulation. All the available sensors are assumed to be working and the determination is initialized from unknown attitude (filter initial guess for quaternion is $\mathbf{q}_{est_0} = [0, 0, 0, 1]$ and for angular velocity is $\boldsymbol{\omega}_{est_0} = [0, 0, 0]$ rad/s). The determination stops and the propagation begins when the spacecraft enters in eclipse and no more data from Sun sensors are available at $t \simeq 650$ s. The convergence of the ADS to the correct values is extremely fast, and the determined attitude is available in less than 10 s, as evident in fig. 5.

Figure 6 reports the angular velocity determination performances. The results presented are related to the same simulation that has been used to discuss about quaternions estimation. In this case, the convergence to the actual value is quite slow because, despite a direct measurement of the angular velocity is always available from the IMU, the bias of the gyroscope is not known and its estimation is indirect. Therefore, in order to use the IMU measurements with the required accuracy, the ADS has to estimate the bias through indirect measurements. The converged result is satisfactory, but is available after 500 s from a completely unknown condition. Nevertheless, the direct angular velocity measures are always available and they can be always used, with an error in the order of the bias of the IMU. It must be remembered, that the bias value is quite stable and constant in time. Hence, once a first estimated bias is obtained within a desired precision, its estimation is not necessary anymore, and the accurate angular velocity determination convergence is faster, because a previously converged bias value can be used as initial condition in the filter.

4. On-board Software

Some of the challenges faced during the software development were tough: from managing the clock cycle to reduce the power consumption up to limit the heat produced by the microcontroller during calculations, everything has to be thought and re-thought several times. In addition to all these difficulties, common during the developing process of a space system, also more application specific ones has been tackled, such as adapt to the developed architecture the ACDS algorithm written and tested only in Matlab/Simulink, as presented in Section 4.3.

4.1 Microcontroller and OS

The final microcontroller embedded in FEES is a STM32L4, an ultra-low-power ARM©32-bit Cortex©-M4 microcontroller. The software development started way before the definitive board was available, so all the preliminary tests were performed on STM DISCO-L476VG,[8] a development board equipped with the same microcontroller of FEES.
The first choice to be made was if using or not an Operative System (OS): if it is true that an OS uses some of the resources available to run itself, it also comes with a lot of low-level functions already implemented, such as a deterministic, multithreaded real time software execution, driver for communication over SPI or I2C and more.

DOI: 10.13009/EUCASS2017-489

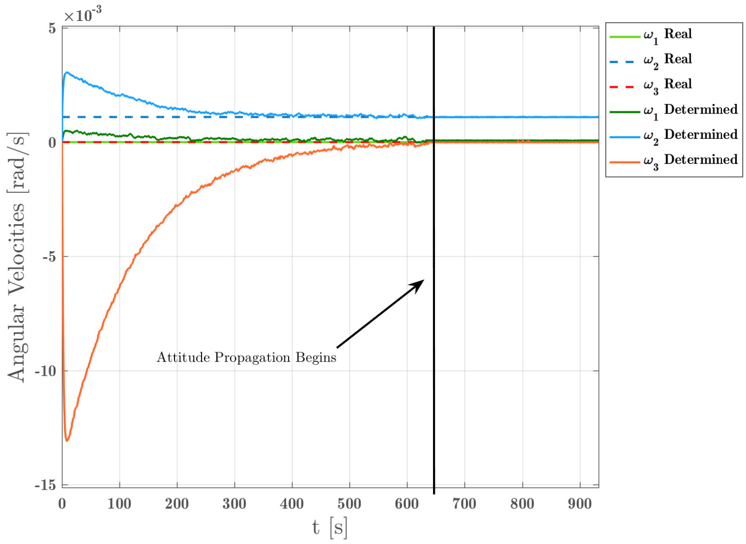

Figure 6: Angular velocities determination performances, starting from unknown angular velocity ω. (Simulation related to the one presented in fig. 5. All the details in the relative caption).

The RTOS (Real Time Operating System) world is wide and presents a lot of possibilities: FEES development choice has fallen upon *mbed OS*,[1] an open source embedded OS. Even though this OS is designed specifically for Internet of Things (IoT), it comes with a set of features helpful for the development purposes: it is based on ARM Cortex-M architecture, the same mounted on FEES on-board system, exploiting all its capabilities. It is secure and it has a fairly good amount of drivers for sensors already implemented. A more detailed discussion about the latter statement will follow in Section 4.2

4.2 Sensors driver

mbed OS has a very large base of supported sensors, but due to its IoT vocation, very few are also suitable for a space-oriented application. This consideration leads to the problem of implementing and testing the driver for each sensor.
The first thing to consider is the stability of the of I2C driver itself. I2C is a serial computer bus used, in general, to attach peripheral to microcontroller for short distance or intra-board communication.
The driver stability is crucial: if the bus cannot handle the amount of information sent by the sensors, a different way round has to be found. The I2C implementation provided by *mbed OS* is robust and reliable: a solid foundation on top of which built the sensor specific driver. Some of the driver needs also further logic in addition at the one handling the transmission of the raw data: some elaborations are needed to get an useful measure (e.g. sun fine-grained sensor)

4.3 ADCS: From Simulink to C++

The core effort of the development was put in the Attitude Determination and Control Subsystem (ADCS) translation from Simulink to C++.
mbed OS, unfortunately, does not provide a mathematic and calculus toolbox: dozens of C++ numerical libraries are available, but their implementation is desktop computer oriented and not with embedded systems in mind.
Therefore the first thing to do was develop a stable and custom math library: this library, called *FEESMath*, provides all the common operations for vectors and matrixes. To avoid cycle and for-loop, the operation are restricted to vectors 3x1 and 4x1 (for quaternions support) and square matrices 3x3 and 4x4.
This choice makes the code more verbose, but it increases its efficiency and performance: no need to exploit branch prediction, the instructions are issued and executed deterministically without problems.
Another advantage of this choice is to maintain memory usage under control: the less the variables are instantiated at runtime, the less easily memory errors happen.
Simulink takes advantage of Matlab core: lot of functions are already implemented and, same way, nuances can be ignored. For instance, low-pass filter can be used by a simple drag and drop, except setting the right parameters of course.
In C++ the same cannot be done: all the details of the filter have to be implemented manually with a constant trade-off

DOI: 10.13009/EUCASS2017-489

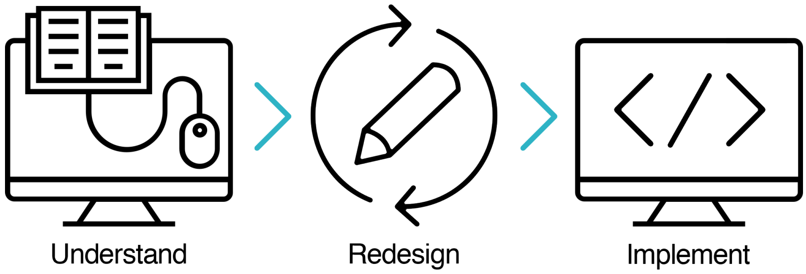

Figure 7: Development phases

between performance, memory and robustness. In fact, a division by zero, handled quite smoothly by Matlab, in an embedded system could lead to serious problem, like crash, if not caught and managed correctly.
Talking about numerical problems, also the floating point precision has to be taken into consideration: by default Matlab uses 64-bit double-floating point precision. This can be changed and conformed to a 32-bit precision, the one supported by available microcontroller, but the Simulink algorithm was thought and tested in double precision: when managing small numbers this difference can lead also to huge errors at the end of the computation.
To conclude, the flow followed in the translation from Simulink to C++ can be summarized in fig. 7: a first phase of understanding the algorithm, then a redesign of it in order to exploit no more Simulink feature, but C++ and custom libraries and eventually the actual implementation. The second phase of redesign is needed also the throw away all those Simulink superfluity: model an if condition or flag is verbose in it while straightforward in C++.

5. TT&C Subsystem

The TT&C subsystem is composed by a set of innovative experimental apparatus. In the frame of the FEES project a new TT&C module has been specifically developed by Linkit srl.[6] The module, with a footprint of only 25 x 38mm is able to provide a maximum datarate of 115 kbps, with the possibility to switch between FSK, GFSK, MSK, GMSK, OOK and even LoRa modulations. The module is half-duplex and has the possibility to operate in two bands: bidirectionally in the amateur range 435-438 MHz and in receiving mode in the amateur range 1260-1270 MHz. The rationale behind this choice is the intense usage of the 435-438MHz band with a related risk of reduced or difficult communication with the satellite. In addition, we have on-board an experimental SDR trasmitter operating on the 435-438 MHz to transmit to ground images taken with a multispectral camera, with different transmission protocols: while the band is occupated by the SDR, we will have still the possibility to command the satellite on the 1260-1270 MHz band in case of emergency. The FEES TT&C module contains a dedicated microcontroller able to switch on/off the radio or activate emergency functions even in case of failure of the main microcontroller, in accordance with international regulations. In the frame of the FEES project Linkit and GP Advanced Projects are developing a dedicated ground station which will be connected and controlled by an Internet application developed by Pandigital srl.[7] Another telecommunication experiment on-board FEES is the presence of an IRIDIUM modem, capable of sending and receiving short data messages. This option will enable FEES to communicate or be commanded in any location independently from the ground stations visibility, capability which is extremely useful in case of LEOP first communication, emergency or communication of real-time data in case of scientific experiments.

6. Power Subsystem

Power subsystem is based on 4 innovative thin solar cells developed and provided by CESI. They are triple junction solar cells InGaP/GaAs/Ge for space applications body mounted on both the large faces of the spacecraft. Each face therefore hosts 2 cells of 26.5 cm^2 in size, for a maximum theoretical available power of 2.1 W per face. The cells efficiency is in about 29%. Moreover, FEES will be equipped with 4 experimental high efficiency InGaAs 2×2 cm^2 solar cells to be tested and space qualified. Just acting as a payload. The bus is regulated at a constant voltage of 3.3 V and the rechargeable battery available on-board is based on Li-Ion with a capacity of 3.5 Ah.

However, the maximum solar power is not available because of the imposed Nadir pointing attitude. Hence, simulations have been carried out to assess the quantity of power available for spacecraft operations and an example result is reported in fig. 8, where the power available while the spacecraft is maintaining the nominal attitude pointing is reported for 5 orbital periods. The solar panel assembly degradation factor has been estimated to be in the order of 0.77 and, thus, each face can produce at maximum 1.6 W, but in nominal attitude the peak power is in the order of 1.4 W

DOI: 10.13009/EUCASS2017-489

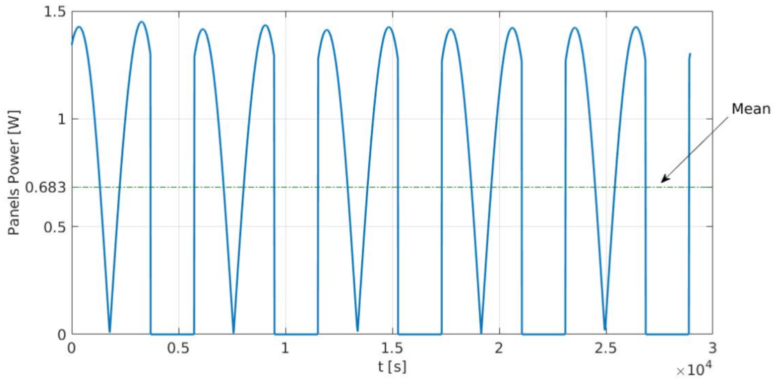

Figure 8: Available solar power in nominal pointing mode.

with a mean value of 0.683 W. Along each orbit the available solar energy is about 300 mAh and the consumed power stays well below this value. Just for reference, the magnetorquers, at maximum during the de-tumbling phase, absorb 5 mAh to stabilize the spacecraft from a completely random spinning condition. The peak power is also sufficient to maintain the system operations; as an example, the maximum power absorbed on-board is below 0.2 W.

After the successful achievement of the primary mission goals, the power available can be maximized activating an alternative guidance in Sun pointing mode. In this case, the ADCS performances are similar, but the operations are more complex and less reliable, because of the slewing needed to correctly orient the antennas. However, in this mission phase the primary objectives are fully satisfied and enhanced operations are possible because of the increased incoming power. In fact, in Sun pointing, FEES panels are able to produce around 475 mAh per orbital period.

7. Structure

FEES structure is designed to withstand the environment's loads and to be compliant with the CubeSat Design Standards (CDS).[11] The main drivers for the design are obviously related to these, but also to electromagnetic compatibility, mass requirements, payload configuration and components accessibility.

As shown in fig. 9 the structure design consists of four 3.8 cm long rails which are in contact with GPOD supports and will slide on them during separation. These rails are connected one another through a series of beams which are used also to attach the external boards.

After few iteration on the design, the selected solution consists in a 3 pieces frame. This result has been achieved starting from the traditional frame consisting in separate beams and rails, by trying to be compliant with TT&C subsystem requirements, to reduce the weight, ease assembly and accessibility. Beams have been removed behind the antennas and structural FR4 boards are considered to maintain the structural rigidity of the entire frame without degrading overall performances.

The main inner board is connected directly to the frame by means of appendages on the rails. Holes at the ends of the rails are present mainly in order to have a faster and easier access to the PCB's screws, but these also help for the outgassing of the internal volume during launch and serve as casing for the spring plunger. These have been positioned only on the opposite longitudinal direction, in compliance with the CDS. All boards, internal and external are joined to the rest of the structure by means of $M3$ titanium screws. Two $M4$ or $M3.5$ stainless steel pin spring plungers are going to be mounted on the previous presented locations.

Moreover, as it can be seen in fig. 9, windows are cut into the rails to house two switches which will power on the

Load	Value
Lateral acceleration	$212\,\mathrm{m/s^2}$
Longitudinal acceleration	$330\,\mathrm{m/s^2}$
Plungers	18 N
Ejection spring	47 N
Other CubeSats	1184 N

Table 1: Loads applied to the structure.

DOI: 10.13009/EUCASS2017-489

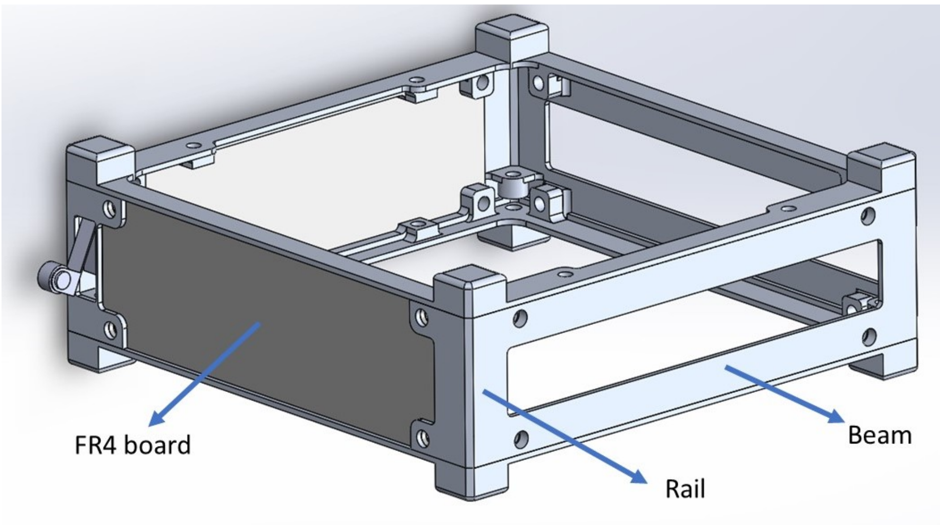

Figure 9: CAD rendering of FEES structure.

spacecraft once it is released. The switches are mounted next to the rails by means of $M2$ screws. A peculiar solution is adopted due to the limited space and the dimension of switches available on the market. OMRON components have been chosen with a roller level. The windows have been designed to allow the lever to be in contact with GPOD's rails and stainless steel rollers have been chosen to reduce the friction during the satellite release and to avoid any cold welding.

The geometrical shape and dimension of beams and rails have been studied in a preliminary, simplified structural analysis aimed to have some insight on the necessary material. This analysis, consisting in modeling rails and beams using De Saint Venant beam theory and thick beam buckling, gave the first approximated dimensions which have been later improved using finer analyses. At this step it was already noted that manufacturability of the structure puts very stringent requirements on the structure, which could be improved, in terms of mass and strength, if new cheap techniques for thin beams manufacture arise. Indeed, it has been observed that the minimum thickness which can be easily manufacture is of 1 mm.

The material chosen for the structure is Al 7075, in compliance to the CDS, resulting in an overall mass of the frame of about 45 g without considering the mass of the switches and screws. This choice was driven from the possibility of having a surface hard anodization and for a satisfactory density over strength ratio with respect to other aluminium alloys.

7.1 Finite element model

To model the structure, a finite element analysis has been set up. A shell model has been created instead of a solid element model to ease the computations while still achieving precision. Contacts have been modeled using frictionless connections and joints have been modeled using deformable beams for screws. To each shell a precise thickness has been prescribed and all the geometries have been linked by means of mesh connection tool. Boards have been simulated by point masses located in PCBs' estimated position of the centre of mass with deformable links.

The created mesh is composed of Tri3 and quad4 elements with a minimum size of 0.15 mm. The total number of elements is 65855, and the corresponding number of nodes is 69900. Mesh quality has been always in mind during the refinement process, by means of localized refinements to ensure proper convergence of calculations. An average mesh quality of 0.88 with a variance of 0.14 has been achieved.

A lot of effort has been put into the choice of the most appropriate boundary conditions for the model and many combinations have been tried. With reference to fig. 10, displacement constraints have been used on the $+Z$, $+X$ and $+Y$ faces of the rails. The reason for these boundary conditions is that the CubeSat rests on the release spring and in contact with the GPOD. Moreover, the boundary conditions have been thought also to ease the testing procedure in laboratory.

Although reasonable, these constraints are not entirely physically correct, and a much more complex analysis would be required for a better modeling. In particular the inaccuracy of this set of constraints arises in the random and modal analyses where the constraints on the $+X$ and $+Y$ faces entirely neglect the small spacing present between the CubeSat and the GPOD. On the other hand removing these constraints implies that the GPOD interface is neglected.

DOI: 10.13009/EUCASS2017-489

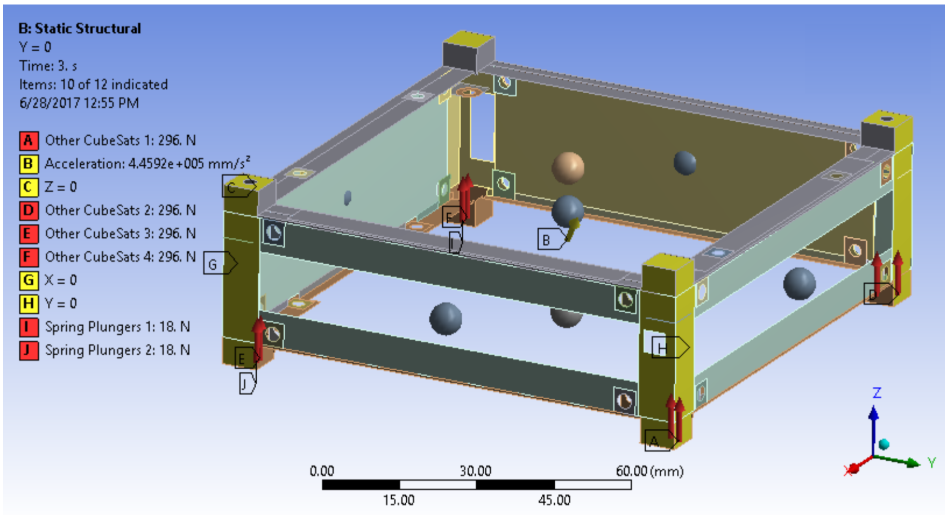

Figure 10: Shell model of FEES structure with applied loads and boundary conditions.

For this reason also other boundary condition configurations have been studied, to ensure the model is sound and results trustworthy.

7.2 Loads

The loads have been set based on the initial launcher specifications, i.e. the DNEPR launcher. Although the launcher has been modified recently, the results can still be considered valid because of the similarities of the applied loads which results lower in the case of Falcon 9 launcher.

The loads acting upon CubeSat have two origins. The first is the inertia contribution due to acceleration of FEES CubeSat, as well as the other CubeSats resting on top of it, whereas the second are the springs that separate and serve as release mechanism. The forces are applied as in fig. 10.

All the loads have been multiplied by a Factor Of Safety (FOS) equal to 1.6, obtained as explained in[15] . Regarding the quasi-static contribution of dynamic loads, Mile's approach has been used using the ASD in the launcher user guide, margined by 3 dB.

7.3 Results

Four different types of analyses have been carried out: static, buckling, modal and random vibration. These all have shown that the designed structure is able to withstand the loads without plastic deformation, confirming the ability of the designed structure to sustain the launch loads. Moreover, the fundamental frequency of the structure results to be higher than the required value from the GPOD requirements. More precisely, it results higher than 400 Hz.

According to our analysis, the most demanding test is the static one which shows a Margin Of Safety of 0.4 related to the FR4 board. Regarding the buckling analysis, it reveals that the MOS is higher than 1.75. Finally, considering a $\pm 3\sigma$ margin, the random vibration MOS results to be 1.28.

These results show that the design can withstand the launch's loads. Future work will be focused on the reduction of the mass of the overall frame without degrading the structural performances. To achieve this result, it is currently under study the possibility to pierce the FR4 boards and to reduce the dimensions of the beams (since it is not technologically possible to reduce the thickness).

8. Final Remarks

This paper was intended to present the FEES picosat mission. The details and the design of the critical on-board subsystems have been discussed, with particular regards to the criticalities that are present while developing such a small platform, extremely limited in mass and volume.

At time of writing, design, test and integration of the small satellite are still on-going processes. Some components are currently being updated because of the recent change of the launcher. As explained in section 7, the Falcon 9 and not the DNEPR has been recently selected from the launch provider to inject FEES in its operational orbit.

DOI: 10.13009/EUCASS2017-489

The proposed system architecture is reliable and effective, and it can be implemented on-board within all the mission constraints. The whole design has followed a practical engineering approach that made available all the parameters of the system immediately usable for verification, integration and testing. The main subsystem components have been designed and integrated on the dedicated motherboard, which can represent the heart of a family of spacecraft with the same electronics but different sizes. Therefore, FEES can be intended as a picosatellite platform scalable and modifiable also for other similar space missions. The performances of all the subsystems are satisfactory and fulfill all the imposed requirements.

Future works will conduct an extensive hardware-in-the-loop verification of the software and the system logic. The system actuation for attitude control has to be tested on ground and the attitude determination section requires the final tuning with all the sensor hardware integrated. The structure will be extensively tested, looking at the new launcher specification. The whole system has to be extensively tested and verified before launch.

9. Acknowledgments

FEES is promoted and developed by GP Advanced Projects in collaboration with other companies and research institutes.

GP Advanced Projects srl has a strong know how in space systems and infrastructures, system engineering and project management activities. In addition, the company has a proven experience in dealing with European companies, institutions, research bodies and space agencies, both European and non-European, and with launch providers. The management responsibility of the FEES project belongs to GP Advanced Projects.[4]

Politecnico di Milano is key actor in space activities, thanks to its participation to some of the most important European and non-European missions. Politecnico di Milano supports FEES in the GNC design, operations and supports the environmental tests in its labs. Moreover, EPS and structure procurement and design are also supported by Politecnico di Milano.

Laser Navigation srl is a company with a proven background of electronic devices design and development, in particular in the Unmanned Aerial Vehicle (drones) sector, where it develops autopilots and control systems. In additions Laser Navigation has a strong know-how in telecommunications and radiofrequency applications. Laser Navigations is in charge of the whole FEES electronics.[5]

CESI is a European leader in the production of solar panel for space application. CESI provides the photovoltaic cells which generates the energy that FEES needs.[2]

LINKIT holds a 20yr experience in the telecommunication and RF field, developing any kind of wireless device. It is in charge of FEES TT&C module.[6]

Pandigital srl, with a consolidated experience in web security and web applications, is developing the ground station remote controlling software and the telemetry database.[7]

Launch brokerage is provided by G.A.U.S.S. srl.[3]

References

[1] ARM mbed OS. *www.mbed.com*.

[2] CESI spa. *www.cesi.it*.

[3] G.A.U.S.S. srl. *www.gaussteam.com*.

[4] GP Advanced Projects srl. *www.gpadvancedprojects.com*.

[5] Laser Navigation srl. *www.radionav.it*.

[6] Linkit srl. *www.linkit.it*.

[7] Pandigital srl. *https://pan.digital*.

[8] STM DISCO-L476VG. *http://www.st.com/en/evaluation-tools/32l476gdiscovery.html*.

[9] Giulio Avanzini, Emanuele L de Angelis, and Fabrizio Giulietti. Acquisition of a desired pure-spin condition for a magnetically actuated spacecraft. *Journal of Guidance, Control, and Dynamics*, 36(6):1816–1821, 2013.

[10] Giulio Avanzini and Fabrizio Giulietti. Magnetic detumbling of a rigid spacecraft. *Journal of guidance, control, and dynamics*, 35(4):1326–1334, 2012.

DOI: 10.13009/EUCASS2017-489

[11] Cal Poly SLO. *CubeSat Design Specifications*.

[12] Andrea Colagrossi, Lorenzo Bucci, Michele Lavagna, and Guido Parissenti. Gnc design and testing for an IOD/IOV 1/3U platform. In *8th European CubeSat Symposium: Nanosatellites for Science and Technology*, 2016.

[13] Andrea Colagrossi, Lorenzo Bucci, Michele Lavagna, and Guido Parissenti. Three-axis active and fully magnetic attitude control design for a 1/3U picosat platform. In *8th Nano-Satellite Symposium (NSAT)*, 2017.

[14] DoD. *MIL-STD-1540C*.

[15] ESA. *ECSS-E-ST-32-10C Rev.1*.

[16] Julie Fagerudd. Stress simulation of the seam cubesat structure during launch. Master's thesis, KTH, 2015.

[17] International Space Company Kosmotras. *Space Launch System DNEPR - User's guide*.

[18] M. H. Kaplan. Modern spacecraft dynamics and control. *New York, John Wiley and Sons, Inc., 1976. 427 p.*, 1, 1976.

[19] Marco Lovera and Alessandro Astolfi. Spacecraft attitude control using magnetic actuators. *Automatica*, 40(8):1405–1414, 2004.

[20] Robert Mahony, Tarek Hamel, and J-M Pflimlin. Complementary filter design on the special orthogonal group so (3). In *Decision and Control, 2005 and 2005 European Control Conference. CDC-ECC'05. 44th IEEE Conference on*, pages 1477–1484. IEEE, 2005.

[21] F Landis Markley. Attitude determination using two vector measurements. 1998.

[22] Bertha Mathieu. Oufti-1 nanosatellite: Dynamic analysis and qualification testing. Master's thesis, University of Liege, 2011.

[23] NASA. *NASA LSP-REQ-317-01A*.

[24] J. R. Wertz. *Spacecraft Attitude Determination and Control*. Kluwer Academic Publishers, Dordrecht, 1990.